Response of a Resistive and Rotating Tokamak to External Magnetic Perturbations Below the Afvén Frequency

M.S. Chu,[1] L.L. Lao,[1], M.J. Schaffer[1] T.E. Evans,[1] E.J. Strait,[1] Y.Q. Liu[2], M.J. Lanctot,[3] H. Reimerdes,[3] Y. Liu,[4] T.A. Casper,[5] and Yuri Gribov[5]

[1]General Atomics, P.O. Box 85608, San Diego, California 92186-5608, USA
[2]Culham Science Centre, Abingdon, Oxfordshire, OX14 3DB, UK
[3]Columiba University, New York, New York, 10027 USA
[4]Dalian University of Technology, Dalean, China
[5]ITER Organization, Route de Vinon sur Verdon, F-13115 Saint Paul lez Durance, France

e-mail contact of main author: chum@fusion.gat.com

Abstract. Recent experiments observed that plasma edge stability can be improved by external magnetic perturbations. The general problem of plasma response to external magnetic perturbations is investigated. Different (vacuum, ideal, and resistive) plasma response models are considered and compared. Plasma response in the edge stability experiments is obtained through computation using the MARS-F code, with a plasma model that includes both plasma resistivity and rotation. The resultant magnetic field line stochsticity is much reduced from that obtained formerly using the vacuum plasma model. This reduced stochasticity is more consistent with the observations during edge stabilization experiments. Examples are given for response of an ITER plasma to perturbations generated by the correction coils; and response of a plasma to external coils (antenna) up to the Alfvén frequency.

1. Introduction and Motivation

Recent experiments in DIII-D [1] and JET have shown that by imposing magnetic perturbations from outside the tokamak, the plasma behavior at the edge can be improved, i.e. the edge localized mode (ELM) stabilized. Vacuum field model of plasma response [2] predicts that field lines on the outside (>90%) flux surfaces of tokamak become stochastic; indirectly supported by the measurment of the splitting of the heat deposition footprint on the divertor plate. However, it resulted in a puzzle because the edge temperature gradient in the experiment was not reduced — which indicated that the heat transport was not much enhanced. This is in direct contradiction with modeling of edge transport using a stochastic edge [3]. On the other hand, the density gradient was slightly reduced in the experiment. An improved magnetic field line structure other than that of the perturbed vacuum field is needed. We propose that the plasma response is essentially ideal and use the MARS-F code [4] to show that the field lines would not become stochastic except at the very edge. We conjecture that this filed line structure will lead to negligible increase in heat transport while slightly increasing the particle transport.

Magnetic perturbations generated by external coils are utilized for various purposes in the study of the tokamak plasmas. At high (Alfvén range) of frequency, they are used to excite plasma waves, whereas at lower frequencies, they are utilized for the correction of error fields and/or for the feedback stabilization of various instabilities including the RWM [5]. One of the intriquing aspect of the above mentioned edge stabilization experiments is that stabilization depends very critically not only on the configuration of the external magnetic coils (and perturbations), but also on the plasma state to which the magnetic pertubation is applied. To extrapolate these effects reliably to future devices,

we need to have a comprehensive understanding of the underlying physical phenomenon and also a simulation capabilty for the combined system of plasma and external coils.

In this work, we compare the plasma response from different (vacuum, ideal, resistive) plasma models and discuss their validity. We showed that the plasma response can be studied through minimizing the free energy of the plasma together with the external coils. In particular, we found that without pitch resonant surfaces, the magnetic plasma response is expected to be slightly paramagnetic with respect to the "response" from the vacuum field. With a pitch resonant surface, the plasma response inside of the resonant surface remains paramagnetic and can be highly amplified; however the magnetic field normal to the flux surface is constrained to be zero at the resonance and thus becomes a diamagnetic response if the ideal plasma model is adopted. Including plasma resistivity relaxes the ideal MHD constraint and brings the response towards the vacuum solution; while rotation reinforces the MHD constraint. To take into account the resistivity and rotation in present day tokamaks, the response is obtained by directly solving the resistive MHD equations using the MARS-F [4] code which also includes the geometry of the external coil(s). Results from MARS-F indicate that the plasma response is very close to being ideal for experimental-like conditions, with only very small amount of flux reconnection over the bulk of the plasma except at the very edge $\sim$2% of the flux surface. The resultant field line topology is not expected to affect the heat transport yet would allow a modest increase to the particle transport, consistent with the experimental observation. Two examples of utility of the magnetic perturbations in understanding the plasma are shown. The first is the perturbation of an equilibrium in ITER by currents in the external correction coils, which can be utilized to counter the effect of the intrinsic error field. The second is obtaining the excitation spectrum and the comparative strength of the excitation by different configurations of the external coils for a plasma and for frequencies up to the Alfvén frequency.

2. Formulation

In present and future tokamaks, plasma resistivity η and equilibrium toroidal rotation Ω are relatively small, i.e. the magnetic Reynolds number $S = \tau_\eta/\tau_H >> 1$ and $\Omega\tau_H << 1$. (Here $\tau_H = R\sqrt{\mu_0\rho}/B$ is the hydrodynamic time and $\tau_\eta = r^2\mu_0/\eta$ is the resistive diffusion time, with R being the major radius, r the minor radius, ρ equilibrium plasma density and B the magnetic field strength.) Therefore, we anticipate that an ideal plasma with no toroidal rotation should be a good first approximation in understanding the response of the plasma to an external magnetic perturbation.

A Response of an Ideal Plasma to External Magnetic Perturbations

The nature of the response of an ideal plasma to external magnetic perturbations may be studied by extending our previous work [6] to include finite perturbation frequency ω. It was shown in Ref. [6] that in the presence of external magnetic perturbations generated by external coils with current I_c, the plasma dynamics obeys the extended MHD functional

$$\delta W_g = \delta K_p(\vec{\xi}^+, \vec{\xi}) + \delta W_p(\vec{\xi}^+, \vec{\xi}) + \delta W_v(\vec{b}_v^+, \vec{b}_v) + \delta E_c = 0 \quad . \tag{1}$$

In Eq. (1), $\delta K_p = \frac{1}{2}\gamma^2 \int dV \vec{\xi}^+ \cdot \vec{\xi}$ is the perturbed plasma kinetic energy; δW_p the perturbed plasma potential energy; δW_v the perturbed magnetic energy in the vacuum region; and δE_c the interaction energy between the coils and the unperturbed equilibrium. The superscript $^+$ indicates the adjoint quantity.

For the "natural oscillations" of an ideal plasma in the absence of the external perturbation coil(s), it is well known that the plasma dynamics satisfy the self adjoint functional $\delta W_I = \delta K_p(\vec{\xi}^+, \vec{\xi}) + \delta W_p(\vec{\xi}^+, \vec{\xi}) + \delta W_v(\vec{b}_v^+, \vec{b}_v) = 0$. At the plasma vacuum interface, the plasma displacement $\vec{\xi}$ and the vacuum magnetic perturbation $\vec{b}_v$ satisfies the connection formula $\vec{\nabla} \times (\vec{\xi} \times \vec{B}) \cdot \hat{n} = \vec{b}_v \cdot \hat{n}$. Here $\hat{n}$ is the outward pointing normal to the edge plasma surface. Without loss of generality, we consider only plasma perturbations with finite perturbation amplitudes at the plasma surface. These perturbations form a set of normal modes $\{\vec{\xi}_i, \vec{b}_{vi}\}$ with the property that $\int dV \vec{\xi}_i^+ \cdot \vec{\xi}_j = \delta_{ij}$; and $\delta W_p(\vec{\xi}_i^+, \vec{\xi}_j) + \delta W_v(\vec{b}_{vi}^+, \vec{b}_{vl}) = -\delta_{ij}\gamma_i^2$. We adopt the magnetostatic representation for the perturbed vacuum magnetic field and express $\vec{b}_i = \vec{\nabla}\Phi_i$. Now we consider the effect of the magnetic perturbation produced by the external coils. The external magnetic perturbation will excite the set of normal modes $\{\vec{\xi}_i, \vec{b}_{vi}\}$ of the plasma to amplitude $\{\alpha_i\}$. Then, the perturbed state of the plasma and the vacuum region can be represeted by

$$\vec{\xi} = \sum_i \alpha_i \vec{\xi}_i \quad ; \qquad \vec{b}_v = \sum_i \alpha_i \vec{\nabla}\Phi_i + I_c \vec{\nabla}\Phi_c \quad . \tag{2}$$

In Eq. (2), Φ_c is the magnetostatic potential of the external coil and satisfies $\nabla^2\Phi_c = 0$. We assume the external coil is located on a coil surface S_c and carrying current I_c. On the surface S_c, the coil current $\delta\vec{j}_c$ can be expressed as $\delta\vec{j}_c = \vec{\nabla}z \times \vec{\nabla}K$ with z being a coordinate perpendicular to the coil surface. Then the magnetostatic potential Φ_c of the coil current satisfies $\Phi_c^+ - \Phi_c^- = \mu_0 \int K dz$ across the coil surface. Because the system of eigenfucntions $\{\vec{\xi}_i, \vec{b}_{vi}\}$ is complete, the boundary condition for Φ_c is $\vec{\nabla}\Phi_c \cdot \hat{n} = 0$. We can evaluate the extended energy functional δW_g to give

$$\delta W_g = \sum_i \left[-\frac{1}{2}(\omega^2 + \gamma_i^2)\alpha_i^+\alpha_i + I_c(\alpha_i^+ E_{ci} + \alpha_i E_{ci}^+) \right] + \frac{I_c^2}{2\mu_0} \int \vec{\nabla}\Phi_c^+ \cdot \vec{\nabla}\Phi_c dV \quad . \tag{3}$$

The minimization of δW_g in Eq. (3) with respect to α_i gives

$$\alpha_i = \frac{I_c E_{ci}}{(\omega^2 + \gamma_i^2)} \quad ; \qquad E_{ci} = \frac{1}{2\mu_0} \int \vec{\nabla}\Phi_i^+ \cdot \vec{\nabla}\Phi_c dV \quad . \tag{4}$$

Thus, the ampltiude of each mode is proportional to both the current in the external coil and E_{ci} and inversely portional to the frequency difference between the external perturbation and the natural frequency of the mode. It is interesting to note that in Eq. (4), the characteristics of the external coils enter only through ω and E_{ci}. E_{ci} depends on the property of the plasma through Φ_i, and it depends on the configuration of the external coils only through Φ_c. We may design to modify the excitation spectrum $\{\alpha_i\}$ through a judicious arrangement of the configuration of the external coil through Φ_c. We note that the ideal plasma model has been found to be a good representation of the linear plasma response for the tokamak over a wide range of plasma operating conditions [7]. Of course, the formula is not applicable to a naturally unstable mode, i.e if $\gamma_i > 0$. Also when the excitation frequency ω coincides with the eigenfrequecy of the plasma $\omega_i = i\gamma_i$, additional physics needs to be included to resolve the singularity [8, 9].

B Response of a Resistive Plasma to External Magnetic Perturbations

With the inclusion of a small resistivity, it is well known that the crucial changes occur at the pitch resonant surfaces in the plasma. At these locations, the ideal MHD constraint of

"frozen in flux" breaks down. The plasma dynamics has to be supplanted by the relaxed constraint of flux reconnection. The essence of this change can be formulated in terms of the generalized energy functional for a force free resistive plasma δW_{pt} [10]. With the substitution of the tearing mode energy functional δW_{pt} for the δW_p, the plasma dynamics can still be cast in the same formalism of δW_g given in Sec. 2A. δW_{pt} is a self-adjoint gauge invariant variational expression with respect to the vector potential $\vec{A}$. It reduces to that of δW_p when the ideal MHD constraint of $\vec{A} = \vec{\xi} \times \vec{B}$ is imposed. δW_{pt} is given by

$$\delta W_{pt}(\vec{A}^+, \vec{A}) = \int dV[(\vec{\nabla} \times \vec{A^+}) \cdot (\vec{\nabla} \times \vec{A}) - \sigma \vec{A^+} \cdot \vec{\nabla} \times \vec{A} - s\vec{B} \cdot \vec{A^+}] \quad . \tag{5}$$

Here $\vec{\nabla} \times \vec{A} = \vec{b}$ is the perturbed magnetic field; $\vec{J} = \sigma \vec{B}$ is the equilibrium current (parallel to the magnetic field). The coefficient of perturbed parallel current s is given by $(\vec{B} \cdot \vec{\nabla})s = -\vec{\nabla}\sigma \cdot \vec{\nabla} \times \vec{A}$. with the solution (in Hamada cooridates V,θ,ζ)

$$s = -P(\vec{B} \cdot \vec{\nabla})^{-1}\vec{\nabla}\sigma \cdot \vec{\nabla} \times \vec{A} - \delta_{nm}\delta(V - V_{n,m})(\vec{B} \cdot \vec{A})_{n,m} exp(in\zeta + im\theta) \quad . \tag{6}$$

In Eq. (6), P stands for the principal part; $V_{n,m}$ the volume enclosed by the pitch resonant (singular) flux surface where $nq = m$, with n being the toroidal mode number and m the poloidal mode number of the perturbation; and $\delta_{n,m}$ is a given constant proportional to the reconnected flux at the singular flux surface.

For tokamaks, σ is of the order of $1/(qR)$. Therefore, in Eq. (5) $\sigma \vec{A^+} \cdot \vec{\nabla} \times \vec{A}$ is of the order of $r/(qR)$ relative to the stabilizing perturbed magnetic energy $\vec{\nabla} \times \vec{A^+} \cdot \vec{\nabla} \times \vec{A}$. If $nq = m$ is never satisfied, then the term proportion to s can be transformed away by choosing a gauge (such as the ideal MHD gauge) for the vector potential $\vec{A}$. In this case, the perturbed potential energy will be dominated by the term of perturbed magnetic energy. Therefore, we obtain the important conclusion that if the external perturbations do not have resonant surfaces in the plasma, the plasma response can be approximated very well by the vacuum response. Also, because the energy of the perturbed magnetic field (even in the plasma region) is always positive, whereas the sign of the σ term is indefinite, the plasma when responding to the external perturbations, will always choose to produce a slightly larger or a paramagnetic reponse than the vacuum response.

However, when the plasma has surfaces that can resonate with the external perturbations, the situation is totally changed. The behavior of the solution actually are separated by the singular surface. Inside and far away from the singular surface, the behavior starts out to be similar to the case of non-resonance and due to the first term on the RHS of Eq. (6), can grow to a very large amplitude. When getting very close to the resonance, the second term of Eq. (6) acts as a constraint on the solution, i.e. it provides a stabilization energy to the solution. The perturbed response is suppressed. In the special case of an ideal plasma, the suppression is complete. We will obtain a smaller or diamagnetic response than that of the vacuum.

The above discussion on the effect of resistivity was for a force free plasma, mainly because the form of the perturbed potential energy can be expressed in an explicitly tractable form as given in Eq, (5). For plasma with finite pressure gradients, the distribution of equilibrium current in the plasma changes from more concentrated on the inboard side of the torus to the outboard side. This will significantly affect the marginal stability of the plasma, i.e. the most unstable mode will change from a kink mode with the largest perturbed amplitude on the inboard side of the torus to a kink-ballooning mode with its perturbed amplitude protruding out on the outboard side. The constrained solution given by Eq. (6) becomes more complicated [11]. Yet, the general discussion of the plasma

response relative to that of the vacuum response remains valid. In other words, we still expect the plasma response to be slightly amplified (paramagnetic) from the vacuum response when there are no resonances in the plasma. Whereas the response is suppressed (diamagnetic) at the singular surfaces when the plasma has a resonance. The suppression is incomplete where plasma resistivity has to be taken into account [10, 11].

C Effect of Rotation and Resistivity —Solution Using MARS-F

Because equilibrium rotation Ω is small, the effect of rotation on the linear plasma response is small when there are no resonances. When there is a resonance, it affects the behavior of the tearing mode and thus the amount of flux reconnection given by δ_{nm} in the previous Sec. 2.B. The analytic behavior of this dependence has been expounded by many authors, see for instance Fitzpatrick [12] for tearing island in cylindric geometry and Smolyakov [13] and Hegna [14] in toroidal geometry. These studies assumed that the coupling of the tearing mode with the rest of the plasma can be cast in terms of simple parameters, such as Δ', the free energy available to drive the tearing mode. In our study, we need to obtain results based on self-consistent values of these parameters and not treat them as unknown. It can only be achieved by detailed modeling through computer simulation using the resistive MHD equations. The MARS-F code[4] solves the following set of resistive MHD equations for the plasma with a sub-sonic toroidal rotation Ω [15].

$$\begin{aligned}
\rho(\tilde{\gamma}+in\Omega)\vec{v} &= -\vec{\nabla}p+\vec{j}\times\vec{B}+\vec{J}\times\vec{b}-\vec{\nabla}\cdot\vec{\pi}-\rho\vec{u}(\vec{v}) \\
(\tilde{\gamma}+in\Omega)\vec{b} &= \vec{\nabla}\times(\vec{v}\times\vec{B}-\eta\vec{j})+(\vec{b}\cdot\vec{\nabla}\Omega)R^2\vec{\nabla}\phi \\
\vec{j} &= \vec{\nabla}\times\vec{b} \\
(\tilde{\gamma}+in\Omega)p &= -(\vec{v}\cdot\vec{\nabla})p-\Gamma P\vec{\nabla}\cdot\vec{v} \quad .
\end{aligned} \tag{7}$$

In Eq. (7), (upper, lower) case symbols are used for the (equilibrium, perturbed) quantities; $(\vec{v},\vec{b},\vec{j},p)$ is the perturbed (velocity, magnetic field, current, pressure). We also used $\frac{\partial}{\partial t}=\tilde{\gamma}=\gamma-i\omega$, and $\frac{\partial}{\partial\phi}=in$. The viscous stress tensor term $\vec{\pi}$ results from fluid approximations to the ion Landau damping and the $\rho\vec{u}(\vec{v})$ is the Coriolis force term.

In the vacuum region external to the plasma, the perturbed magnetic field satisfies $\vec{\nabla}\cdot\vec{b}=0$ and , $\vec{j}=\vec{\nabla}\times\vec{b}/\mu_0$ with μ_0 normalized to 1. $\vec{j}$ is given by the external current source at the location of the external coil and 0 everywhere else.

3. Simulation Results at Zero Frequency

A Verification of MARS-F with SURFMN

One of the most important results from previous studies on the plasma response to external perturbation during the ELM stabilization experiment was obtained by the SURFMN code [2]. SURFMN computes B field from real 3D coil geometry by integrating the Biot-Savart formula for the currents and its helical Fourier harmonics. Due to its simplicity and versatitily in modeling the coil structure, SURFMN was extremely useful in correlating a number of experimental observations. From the discussion in Sec. 2B, we see that it is also a good approximation for the non-resonant response. Over the whole cross-section of the plasma, the results from SURFMN can be represented by Fig. 1.

Figure 1(a) is the contour plot of b_{m3} for the perturbed magnetic field. The horizontal axis is the poloidal mode number m. Negative m are left- and positive m are right-handed helical harmonics. Figure 1(b) shows the calculated magnetic island widths. For

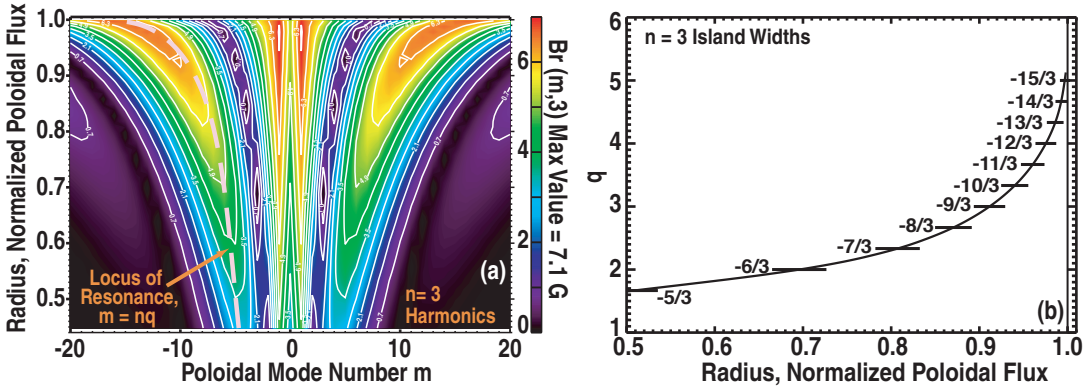

FIG. 1. (a) Contour plot of b_{m3} for the perturbed magnetic field in a DIII-D ELM suppression experiment. The horizontal axis is the poloidal mode number m. Negative m are left- and positive m are right-handed helical harmonics. (b) Calculated magnetic island widths. Note that the outermost 12% of the plasma satisfies the island overlap criterion and the field becomes stochastic.

any resonant plasma surface, the width of the magnetic island in poloidal flux is computed using the formulae

$$w_\psi^{mn} = \sqrt{16\frac{q}{q'}\tilde{\psi}^{mn}} \quad ;\tilde{\psi}^{mn} = \frac{Sb_\perp^{mn}}{2m\pi^2} \quad ;b_\perp^{mn} = \frac{2\int b_\perp exp(i(m\theta_{pest} - n\phi))da}{\int da} \tag{8}$$

In Eq. (8), da is the surface area element of the flux surface; S the surface area. $\tilde{\psi}^{mn}$ is the usual perturbed flux. It is noted that the outer most 12% in poloidal flux of the plasma satisfies the island overlap criterion and field lines become stochastic.

Because many experimental phenomea have already been compared against results from SURFMN, the first step of our study was to verify that results from MARS-F, neglecting the effect of plasma, agrees with that from SURFMN.

We proceed by formulating the vacuum response problem independently by using an analytic method and test it against the the two numerical codes. Results from MARS-F and SURFMN are found to give excellent agreement with the analytic method. This validated results from both codes.

B MARS-F Results with the Inclusion of Resistivity and Rotation

Next the same plasma analyzed in Sec. 3A is tested for various resistivity and flow profiles (including the profiles in the experiment) and external coil configurations. The results are shown in Fig. 2, where we compare the amplitudes of the resonant and non-resonant harmonics of the perturbed normal magnetic field b_n for various levels of plasma resistivity (with magnetic Reynolds number ranging between $S = 10^6$ to 10^8) and also with cases of an ideal plasma (blue) and with vacuum (red). The non-resonant harmonics of $m = 10$ and $m = 12$ are shown in Fig. 2(a); and the resonant harmonics of $m = -10$ and $m = -12$ are shown in Fig. 2(b). We note that overall, the resistive plasma response is very similar to an ideal plasma and deviates from the vacuum. For the non-resonant components, the ideal response is slightly larger (paramagnetic) than the vacuum solution and almost independent of resistivity. Whereas for the resonant components, the response is suppressed at the resonant surfaces, with complete suppression (or shielding) for the ideal plasma. With added plasma resistivity, the shielding becomes imperfect. But with

experimentally measured rotation profile and with a wide range of plasma resistivity, the shielding remains substantial. The presented physical picture is very similar to the conclusion by Izzo and Joseph [16]. These results also agree with the qualitative analysis presented in the previous section. In comparison to the vacuum response, the size of magnetic island, which is proportional to $\sqrt{b_n}$ at the resonant surfaces is much reduced and would not expect to lead to field line stochasticity, except at the last 2% of the flux surfaces.

Similar results were found for different plasma shapes with various plasma elongations and triangularities. We thus conclude that with the level of rotation observed in DIII-D, we would not expect the edge to be stochastic.

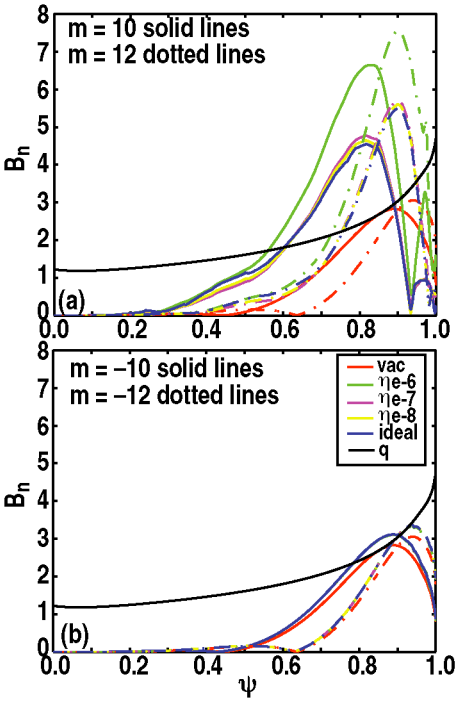

FIG. 2. Comparison of the amplitude of the resonant harmonic components of the pertubed normal magnetic field for a DIII-D plasma with an $n = 3$ perturbation field for a range of the resistivity with that of an ideal plasma (blue) and vacuum (red). It is seen that the plasma response behaves more like an ideal plasma and deviates quite subatantially from a vacuum. In (a) are the resonant harmonics and in (b) the non-resonant harmonics.

C Application to Error Correction in ITER

Complete axisymmetry is an idealization. There will be inherent non-axisymmetry from the non-perfect alignment of the equilibrium producing and maintenance coils. These non-perfections have to be minimized to ensure successful operation of the experiments. In ITER, correction coils have been designed for error field correction. The correction coils should produce external magnetic fields with an effect on the plasma

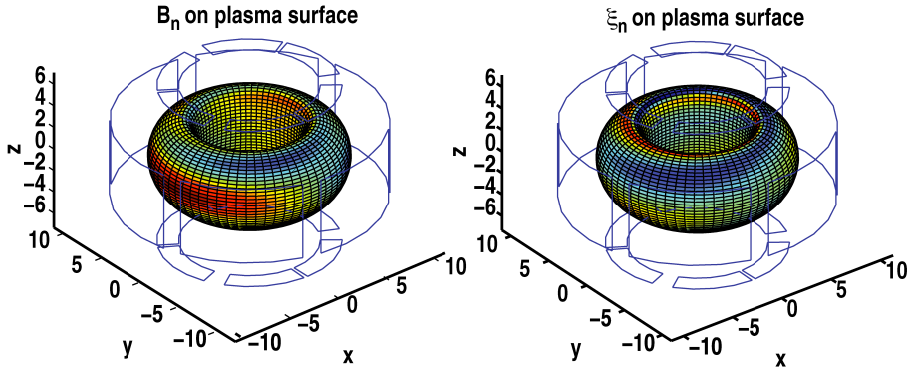

FIG. 3. (a) $n = 1$ perturbed magnetic field on the plasma surface for a low β ITER plasma. Here, the external magnetic field is produced by the side correction coil. (b) $n = 1$ perturbed displacement on the plasma surface. Correction coils are represeted by the external blue lines.

opposite to that of the intrinsic error field. Therefore, by studying the effect of the perturbations on the plasma by these correction coils, we will be able to know the kind of intrinsic error fields that can be corrected by them. Shown in Fig. 3 is, on the left, the

perturbed normal magnetic field on the plasma surface produced by the side-correction coils on a low β plasma in ITER. On the right, the corresponding induced plasma displacement. It is interesting to note that although the magnetic perturbations from the external fields are achiral, the plasma displacements do have a net helicity content.

4. Plasma Response at Higher Frequencies

At higher frequencies, the plasma response is relevant for the study of various plasma eigenmodes such as the TAE, RSAE etc. We applied the MARS-F code to study the plasma response as a function of freqeuncy ω. We found that at a certain set of frequencies $\{\omega_i\}$, the plasma will respsond with very large amplitude, measured for instance by a large kinetic energy δK. As mentioned in Sec. 2A, we need to introduce artificial damping to resolve these singularities. We follow the work in Ref. [8] by introducing a complex frequneny into the driving frequency, these response peaks become broadened and resolved. The width of these response peaks can be related to the continnum damping [8]. They can also be obtained by using the method of adding plasma resistivity [9]. We used two different configurations for the external coils in this study. The ratio of the kinetic energy response from the plasma to the energy input from the external coils is plotted as a function of frequency in Fig. 4. It is seen that the set of frequencies $\{\omega_i\}$ at which the plasma responds with large kinetic energy δK is independent of the excitation geometry of the external coils, but the amplitude could be very different. This is in agreement with the results presented in Sec. 2A.

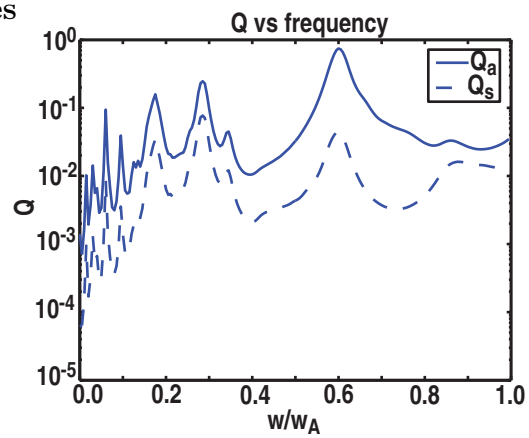

FIG. 4. $Q = \frac{\delta K}{P}$ where δK is the total kinetic energy of the plasma and P is the Poynting flux from the excitation coils for the plasma vs excitation frequency for current arrangement in the I-coils in DIII-D. Q_s for up-down symmetric currents and Q_a for up-down asymmetric currents.

Work Supported in part by US DOE under DE-FG02-95ER54309 DE-FG02-89ER53297 and by the ITER Organization uner Task Agreement C19TD31FU.

References

[1] EVANS, T.E., et al., Nucl. Fusion **45** (2005) 595
[2] SCHAFFER, M.J., et al., Nucl. Fusion **48** (2008) 024004
[3] JOSEPH, I., et al., , J. Nucl. Mater. **363-365** (2007) 591
[4] LIU, Y.Q., et al., Phys. Plasmas **7** (2000) 3681
[5] CHU, M.S. and OKABAYASHI, M., Plasma Phys. Control. Fusion, accepted(2010)
[6] CHU. M.S., et al., Nucl. Fusion **43** (2003) 441
[7] LANCTOT, M.J., et al., Phys. Plasmas **17** (2010) 030701
[8] VILLARD, L., et al., Compter Phys. Reports **4** (1986) 95
[9] KERNER, W., et al., J. Comp. Phys. **142** (1998) 271
[10] CHU, M.S., et al., Phys. Fluids **B1** (1989) 62
[11] CHU, M.S., et al., Phys. Fluids **B5** (1993) 1593
[12] FITZPATRICK, R. and HENDER, T.C., Phys. Fluids **B3** (1991) 644
[13] SMOLYAKOV, A.I., Plasma Phys. Control. Fusion **35** (1993) 657
[14] HEGNA, C.C., Phys. Plasmas **6** (1999) 3980
[15] CHU, M.S., et al., Phys. Plasmas **2** (1995) 2236
[16] IZZO, V. and JOSEPH, I., Nucl. Fusion **48** (2008) 11504